

The **next generation** GBCA  
from Guerbet is here

Explore new possibilities >

Guerbet | 

© Guerbet 2024 GUOB220151-A

# AJNR

## **Use of CT Angiography in Comparison with Other Imaging Techniques for the Determination of Embolus and Remnant Size in Experimental Aneurysms Embolized with Hydrogel Filaments**

This information is current as of July 19, 2024.

M. Killer, M.R. McCoy, M.C. Vestal, L. Weitgasser and G.M. Cruise

*AJNR Am J Neuroradiol* 2011, 32 (5) 923-928

doi: <https://doi.org/10.3174/ajnr.A2554>

<http://www.ajnr.org/content/32/5/923>

ORIGINAL  
RESEARCH

M. Killer  
M.R. McCoy  
M.C. Vestal  
L. Weitgasser  
G.M. Cruise



# Use of CT Angiography in Comparison with Other Imaging Techniques for the Determination of Embolus and Remnant Size in Experimental Aneurysms Embolized with Hydrogel Filaments

**BACKGROUND AND PURPOSE:** Beam-hardening artifacts in CTA can be greatly reduced by using metal-free coils for aneurysm embolization. We compared the embolic masses and remnants of experimental rabbit aneurysms coiled with hydrogel filaments by using DSA, CTA and histology.

**MATERIALS AND METHODS:** Embolization of 12 rabbit bifurcation aneurysms was performed with detachable hydrogel filaments. Six aneurysms were embolized as completely as possible, and 6 aneurysms were embolized incompletely to intentionally leave remnants. Three aneurysms in each group underwent follow-up at 4 and 13 weeks. DSA, MRA, and CTA were performed immediately before sacrifice. The harvested aneurysms were evaluated histologically. For each imaging technique, the areas of the embolic mass and remnant were determined by using image analysis. Results were compared by using paired *t* tests.

**RESULTS:** CTAs were suitable for quantification of the embolus and remnant areas because only small streaking artifacts were evident. The areas of the embolus were larger on CTA compared with DSA and histologic sections. The areas of the remnant were larger on CTA and MRA compared with DSA and histologic sections. Like DSA and MRA, CTA was suitable for determining whether aneurysm retreatment was necessary, provided that loops of hydrogel filaments were not present in the parent artery.

**CONCLUSIONS:** We demonstrated that CTA is a technique with potential for surveillance of aneurysms treated with hydrogel filaments. Additional work is required to determine the accuracy of the technique compared with currently accepted imaging modalities of DSA and MRA.

**ABBREVIATIONS:** CCA = common carotid artery; CTA = CT angiography; DSA = digital subtraction angiography; HU = Hounsfield unit; MRA = MR angiography

Endovascular embolization of intracranial aneurysms with platinum coils and platinum-polymer hybrid coils has become an accepted treatment method to prevent hemorrhage.<sup>1-3</sup> However, drawbacks of the endovascular treatment method are aneurysm recurrence, coil compaction, and recanalization, particularly in large aneurysms or aneurysms with large necks.<sup>4,5</sup> Long-term surveillance is therefore required to determine if additional treatment of the aneurysm is necessary.

While there is widespread agreement that endovascularly treated aneurysms require surveillance, several imaging options are available. DSA is the standard technique used for imaging coiled aneurysms. However, DSA is an invasive catheter-based procedure, requires time, and has potential complications.<sup>6,7</sup> MRA is being increasingly used to conduct follow-up of coiled aneurysms to determine occlusion.<sup>8-10</sup> MRA is noninvasive; however, it is contraindicated for patients with pacemakers and other biostimulators.

Another potential imaging technique for aneurysm surveillance is CTA. It is an inexpensive noninvasive imaging technique with widespread availability and short examination times. While CTA has been increasingly used for the surveillance of clipped aneurysms,<sup>11</sup> the beam-hardening artifacts of platinum coils preclude its use for the surveillance of coiled aneurysms.<sup>12,13</sup> If these artifacts could be reduced or eliminated through modifications of the imaging technique<sup>14</sup> or change of embolization materials, CTA would be a useful technique for coiled aneurysm surveillance, particularly considering the increasing use of stents in conjunction with embolization coils.

Recently DSA- and CTA-compatible hydrogel filament embolic devices have been reported.<sup>15</sup> These hydrogel filaments are metal-free; thus, the beam-hardening artifacts are greatly reduced. The purpose of our study was to demonstrate that CTA could be used to evaluate aneurysm occlusion in experimental rabbit bifurcation aneurysms embolized with hydrogel filaments and to compare the areas of the embolic mass and aneurysm remnant when the experimental aneurysms were studied with DSA, CTA, MRA, and histologic sections.

## Materials and Methods

### Experimental Design

The rabbits were cared for in accordance with Austrian regulations governing animal experiments, and the experimentation was approved by the committee for animal experiments from Land Salz-

Received July 10, 2010; accepted after revision September 30.

From the Neuroscience Institute/Department of Neurology (M.K., L.W.) and Department of Radiology and MRI (M.R.M.), Paracelsus Medical University, Christian Doppler Clinic, Salzburg, Austria; and MicroVention Terumo (M.C.V., G.M.C.), Tustin, California.

This work was funded by MicroVention Terumo, Tustin, California.

Please address correspondence to Monika Killer, MD, Neuroscience Institute/Department of Neurology, Paracelsus Medical University, Christian Doppler Clinic, Ignaz Harrer Str 79, A-5020 Salzburg, Austria; e-mail: m.killer@salk.at



Indicates open access to non-subscribers at [www.ajnr.org](http://www.ajnr.org)

DOI 10.3174/ajnr.A2554

**Table 1: Procedural results<sup>a</sup>**

	Complete Embolization (n = 6)	Incomplete Embolization (n = 6)
Dome (mm)	4.2 ± 0.8	5.0 ± 1.6
Length (mm)	9.0 ± 2.1	10.5 ± 1.1
Neck (mm)	3.8 ± 1.2	4.2 ± 1.9
Volume (cm <sup>3</sup> )	0.13 ± 0.06	0.22 ± 0.14
Number of devices	4.3 ± 2.9	3.7 ± 1.6
Device length (cm)	36 ± 17	34 ± 16

<sup>a</sup> Statistically significant differences between the groups were not observed.

burg, Austria. Experimental bifurcation aneurysms were created in 12 New Zealand white rabbits (mixed sex, 2.5–3.5 kg). Three weeks post-creation, the aneurysms were embolized with detachable hydrogel filaments. Six aneurysms were embolized as completely as possible. Six aneurysms were embolized incompletely to ensure blood filling in the neck. Three aneurysms from each group underwent DSA, CTA, and MRA follow-up and harvest at 4 and 13 weeks.

### Aneurysm Creation

Experimental bifurcation aneurysms were created in 12 New Zealand white rabbits. The microsurgical construction of the carotid bifurcation aneurysms was performed according to previously described methods.<sup>16</sup> Both CCAs were exposed, and a permanent ligature was placed proximal to the left CCA bifurcation and transected. With single-knot 10-0 Prolene sutures (Ethicon, Cincinnati, Ohio), an end-to-side anastomosis of the left-to-right CCA was performed, and the aneurysm sac was constructed with a venous graft pouch from the left external jugular vein. For all operative procedures, the animals were anesthetized by using an intramuscular injection of 20–30 mg/kg of ketamine hydrochloride and 0.2 mL of 2% xylazine hydrochloride, followed by maintenance anesthesia with intravenous injection of a saline solution of ketamine and xylazine (5:1:5; 0.5–1 mL/h/kg).

### Embolic Devices

Detailed descriptions of the preparation, characterization, and physical evaluation of the hydrogel filaments is given elsewhere.<sup>17</sup> Briefly, the hydrogel filaments comprised 66% barium sulfate, 23% trimethylolpropane ethoxylate triacrylate, 8% tert-butyl acrylate, 2% 2-hydroxyethyl methacrylate, and 1% N,N'-methylenebisacrylamide. Filaments of various secondary diameters (2–6 mm and straight) and lengths (4–20 cm) were used to embolize the aneurysm sac. The hydrogel filaments underwent a 1.4-fold increase in volume on hydration.

### Aneurysm Embolization and Follow-Up

With the rabbit under anesthesia and with sterile conditions, the right femoral artery was surgically exposed and a 5F vascular sheath was placed. Following intravenous heparin (100 U/kg) administration, a 5F guiding catheter was advanced into the right CCA. The aneurysm dimensions were measured by using DSA with a radiopaque ball bearing (7.9 mm) as a sizing reference. A microcatheter was advanced into the aneurysm sac.

Embolization was performed under fluoroscopic guidance. Six aneurysms were embolized as completely as possible while minimizing protrusion of embolic devices into the parent artery. The distal half of the remaining 6 aneurysms was embolized, ensuring blood filling in the neck of the aneurysm. After performing DSA to document contrast filling into the aneurysm sac, we removed all catheters and the sheath. The proximal aspect of the femoral artery was ligated with 6-0 silk suture.

At the time of follow-up, the rabbits were anesthetized and a 5F sheath was placed in the left femoral artery. Follow-up angiography was performed by using a 5F guiding catheter positioned in the right CCA. Following DSA, the rabbits were imaged by using CT and MR imaging. They were sacrificed by a lethal injection of sodium pentobarbital or an overdose of the anesthetic agents and 2 mL of T61 euthanasia solution.

### CTA

CTA was performed by using a 10-multisectional helical CT machine (Brilliance 10; Philips Healthcare, Best, the Netherlands). With a power injector, contrast (10 mL, 80% Visipaque 270:20% 0.9% saline; GE Healthcare, Piscataway, New Jersey) was administered through a cannula in the ear vein of the rabbit at a rate of 0.5 mL/s. CTA was performed (0.9–120 kV, 250 mAs, 10 × 0.8 mm) by using a bolus-triggered system with 110-HU threshold through a transverse section at the level of the heart. Postprocessing was performed on a workstation (Brilliance, Philips Healthcare) for viewing multiplanar reformatted images. Using the DSA image as a reference, we prepared 2D maximum intensity projection views.

### MRA

Initial unenhanced MRA was performed by using a 3T scanner (Magnetom Trio; Siemens, Erlangen, Germany) with the rabbit placed inside a 32-channel head coil (Siemens). The aneurysms were imaged by using a 3D time-of-flight sequence with a TR of 23 ms, a TE of 4.37

**Table 2: Quantification results**

Rabbit Group	Embolic Mass Area (mm <sup>2</sup> )			Remnant Area (mm <sup>2</sup> )			
	DSA	CTA	Histology	DSA	CTA	MRA	Histology
Incomplete embolization							
1	14.1	41.1	18.5	25.9	0.0	25.1	21.0
2	23.7	52.9	23.5	16.5	6.1	25.5	13.5
3	42.0	66.7	21.0	33.5	20.3	43.5	19.5
4	33.1	81.2	33.7	33.1	6.1	48.2	8.3
5	24.1	33.5	23.0	10.4	10.5	13.6	6.5
6	14.7	42.1	18.1	16.2	6.4	17.5	7.7
Complete embolization							
7	27.0	48.7	25.4	1.1	0.0	2.5	0.1
8	11.1	32.2	12.9	1.4	0.0	3.9	0.9
9	36.7	60.5	23.6	9.3	0.0	11.8	8.0
10	23.1	27.6	18.2	3.1	0.0	5.8	6.6
11	41.3	88.2	37.9	5.0	0.0	7.8	6.4
12	51.9	58.4	29.6	0.0	0.0	6.3	0.4

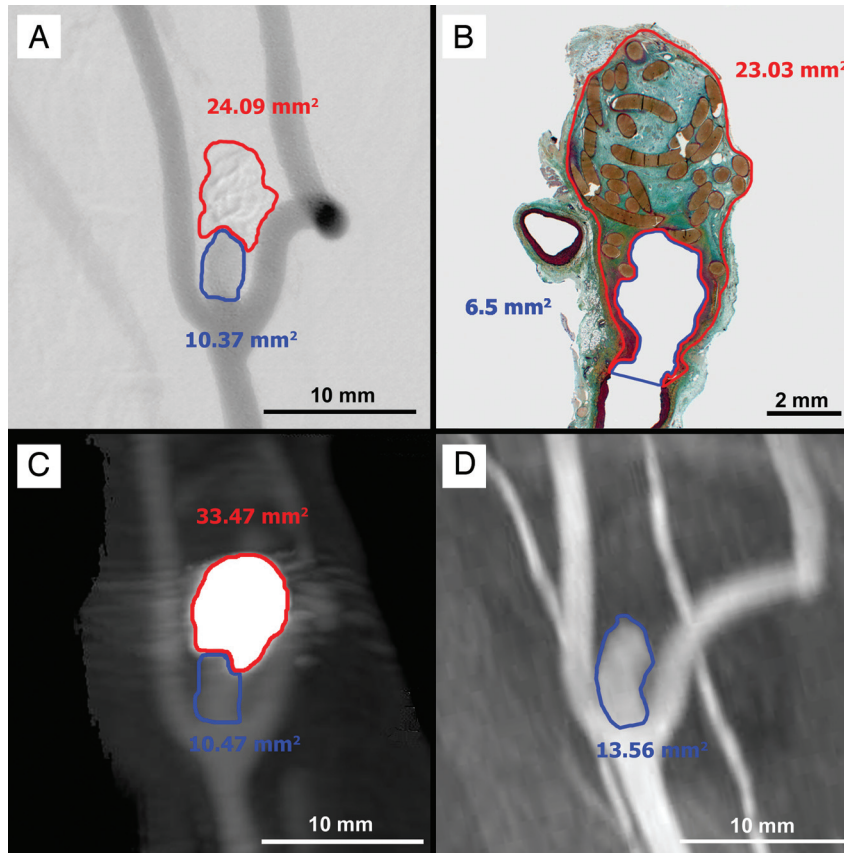


**Fig 1.** Example of image quantification. DSA (A), histologic (B), CTA (C), and MRA (D) imaging of an experimental aneurysm with incomplete occlusion showing the embolus (red outline) and neck remnant (blue outline).

ms, a flip angle of  $18^\circ$ , a matrix of  $304 \times 384$ , an FOV of  $150 \times 150$  mm, and a voxel size of  $0.4 \times 0.4 \times 0.6$  mm. MRAs were prepared on a workstation (syngo MR B15, Siemens) by using the DSA image as a reference.

### Histologic Processing

The aneurysm–parent artery complex was first rinsed in situ with saline solution and then perfusion-fixed with 10% neutral buffered formalin. After surgical excision, the specimen was placed in fresh fixative. To preserve the hydrogel filament–tissue interface, we embedded 6 of the aneurysms in methyl methacrylate. The aneurysms were sawed longitudinally through the neck and  $6\text{-}\mu\text{m}$  sections were prepared by using a rotary microtome. To permit immunohistochemical analyses, the remaining 6 aneurysms were embedded in paraffin and then bisected longitudinally through the neck of the aneurysm. Five-micrometer sections were prepared by using a rotary microtome. The methacrylate and paraffin sections were stained with hematoxylin and eosin and Movat pentachrome stains.

### Evaluation Criteria

**Procedural.** Using the pre-embolization angiogram with the external sizing device, the aneurysm dome, length, and neck were recorded. The volume of the aneurysm was calculated from the dome and length assuming cylindrical geometry. Additionally, the number of devices and the total device length were recorded.

**Quantification.** Follow-up angiograms underwent occlusion quantification.<sup>18</sup> The embolus and remnant areas were determined by using image-analysis software (AxioVision 4.6; Carl Zeiss Microim-

aging, Thornwood, New York). Any contrast filling (DSA/CTA) or blood flow (MRA) inside the aneurysm sac was presumed to be an aneurysm remnant. Embolic devices located outside the aneurysm sac (ie, in the parent artery) were ignored. The area of the embolic mass on MRA was not quantified because it was not visible.

For each aneurysm, the histologic section best illustrating the neck underwent computerized morphometry quantification.<sup>18</sup> The sections were photographed by using an AxioCam MRC5 digital camera mounted on an Axio Imager A1 microscope with a 1.25X objective and were analyzed by using AxioVision software (Carl Zeiss Microimaging, Germany). The embolus and remnant areas were quantified. The remnant was defined as all open spaces contiguous with the parent artery.

### Statistical Analysis

Statistical analyses were performed by using JMP 7.0 (SAS Institute, Cary, North Carolina). For the procedural data, differences in continuous and discrete data were assessed by using analysis of variance and  $\chi^2$  tests, respectively. The embolic mass and remnant areas were compared by using paired *t* tests. Statistical significance was accepted at  $P \leq .05$ .

### Results

#### Procedural

All 12 aneurysms were successfully embolized. All rabbits were in good health without any observable neurologic deficit during the course of the experiment. The procedural results are

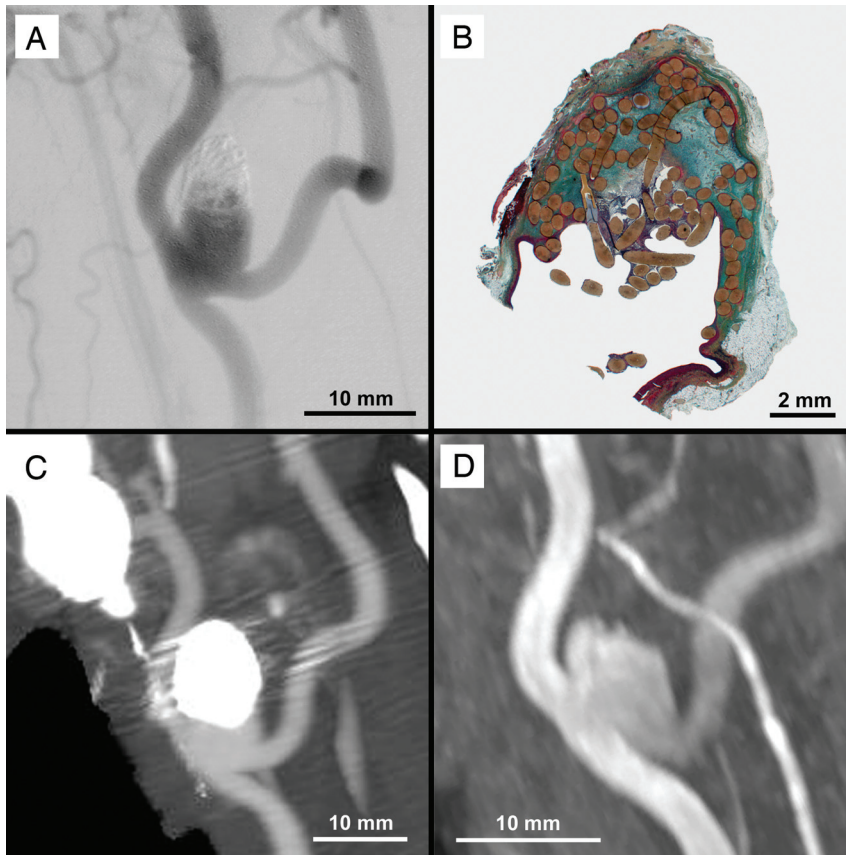


**Fig 2.** DSA (A), histologic (B), CTA (C), and MRA (D) imaging of an experimental aneurysm with incomplete occlusion.

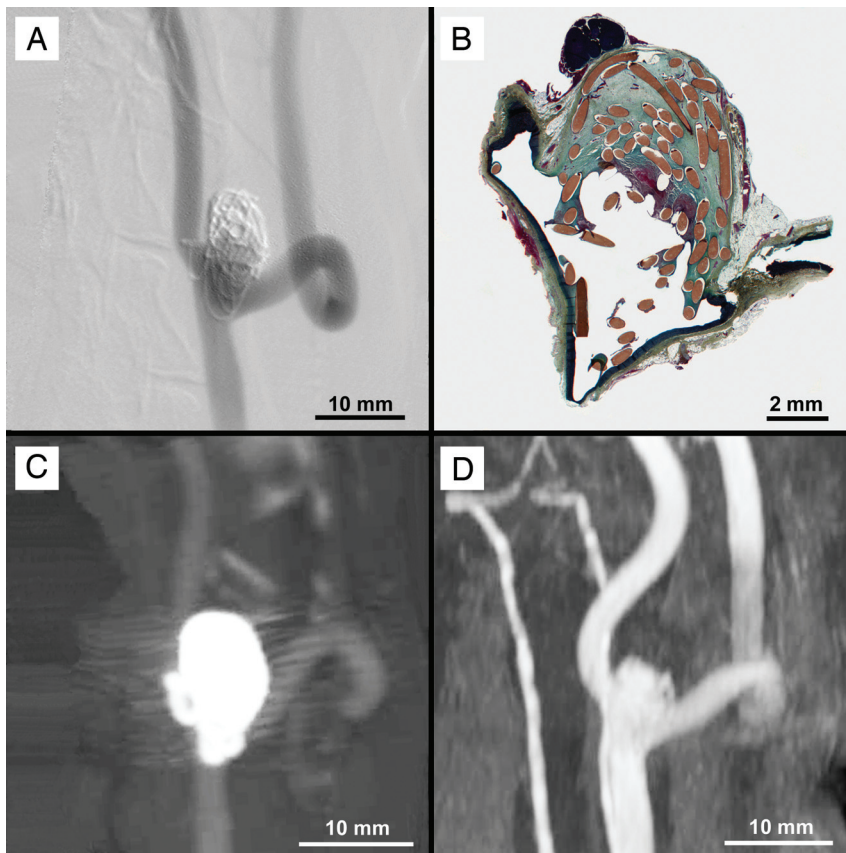


**Fig 3.** DSA (A), histologic (B), CTA (C), and MRA (D) imaging of an experimental aneurysm with near-complete occlusion.

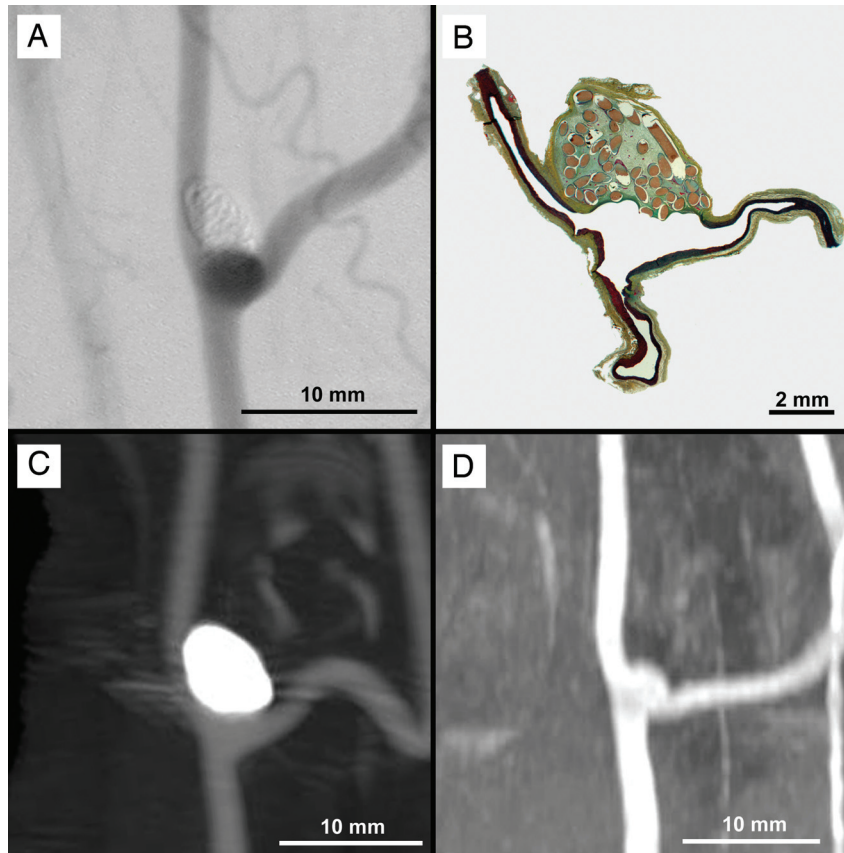


**Fig 4.** DSA (A), histologic (B), CTA (C), and MRA (D) imaging of an experimental aneurysm with complete occlusion.

summarized in Table 1. Statistically significant differences in the procedural results between the 2 groups were not observed.

#### Quantification

The quantification results of the DSA, CTA, MRA, and histologic sections are presented in Table 2. In the matched-pair analysis of the embolic mass area, the CTA areas were significantly higher than the DSA ( $P = .0028$  and  $P = .02$ ) and histologic section ( $P = .004$  and  $P = .005$ ) areas for both the incomplete and complete embolization groups.

In the matched-pair analysis of the incomplete embolization group, the remnant area of the MRA was significantly higher than that of the CTA ( $P = .02$ ) and histologic sections ( $P = .03$ ). Additionally, the remnant area of the DSA was significantly higher than that of the CTA ( $P = .02$ ) and histologic sections ( $P = .03$ ). In the complete embolization group, the remnant area of the MRA was significantly higher than that of the DSA ( $P = .007$ ), CTA ( $P = .005$ ), and histologic section ( $P = .04$ ) areas.

#### Discussion

In this study, we demonstrated that experimental aneurysms embolized with hydrogel filaments had only minimal beam-hardening artifacts when imaged with CTA, without manipulation of the acquisition or reconstruction parameters. We then evaluated the accuracy of CTA in comparison with DSA, MRA, and histology by determining the areas of embolus and remnant. The beam-hardening artifacts of the hydrogel fila-

ments were greatly reduced compared with platinum coils, though some artifacts remained. While vascular pulsation exaggerates the beam-hardening artifacts, we believe that the bulk of the residual artifacts was from the barium sulfate in the hydrogel filaments.

The area quantifications of the embolus by using CTA of both the incomplete and complete embolization groups were generally larger than those on DSA and histologic sections. These results are consistent with those of previous reports comparing volume measurements by using DSA and CTA of silicone aneurysm models.<sup>19,20</sup> These in vitro experiments demonstrated that CTA overestimated the volume of the aneurysms.

The area quantifications of the remnant on MRA of both the incomplete and complete embolization groups were generally larger than those on DSA and histologic sections. These results are inconsistent with those of a previous report comparing volume measurements by using DSA and MRA of silicone aneurysm models,<sup>19</sup> in which MRA measurements resulted in smaller volumes relative to DSA. The reasons for this difference are unknown but may be related to the complexities imparted by the use of animal models and embolized aneurysms.

The area quantifications of the remnant on histologic sections of both the incomplete and complete embolization groups were generally equivalent to those on DSA. Because we attempted to prepare the section through the neck of the aneurysm without regard for the CTA, DSA, or MRA imaging plane, the largest cross-section of the aneurysm was evaluated.

Because adjacent planes shaded the plane of interest on DSA, essentially the largest cross-section of the aneurysm was displayed when it was imaged with DSA.

This study, although demonstrating the potential application of CTA in aneurysm surveillance, had limitations. First, because this study was a comparison of quantified areas of DSA, CTA, MRA, and histologic sections, it was dependent on obtaining images from approximately the same plane for accurate analyses. As Figs 1–4 show, we were reasonably successful at matching the plane for the DSA, CTA, and MRA analyses. Due to the nature of the histologic processing, we could not match the plane of analysis and were limited to the section produced. Second, the number of aneurysms in each group was small. Six experimental aneurysms were incompletely embolized, and 6 aneurysms were completely embolized. The accuracy of the use of CTA in aneurysm follow-up has not yet been established. Additional larger studies are required to determine its accuracy.

## Conclusions

We demonstrated that CTA could be used to evaluate occlusion of aneurysms embolized with hydrogel filaments. CTA overestimated the size of the embolus and remnant compared with DSA, MRA, and histologic sections. CTA provided imaging suitable for determining whether retreatment was necessary, except in the cases in which hydrogel filaments protruded into the parent artery. With improvement in the design of the hydrogel filaments, the advantages of aneurysm surveillance with CTA could be realized.

## Acknowledgments

We gratefully acknowledge the contributions of Drs T. Hauser, R. Agic, M. Kral, and A. Wallner in conducting the preclinical studies and the contributions of M. Schober and E.M. Reiter in conducting the CTA and MRA imaging.

## References

1. Molyneux AJ, Kerr RS, Yu LM, et al. **International Subarachnoid Aneurysm Trial (ISAT) of neurosurgical clipping versus endovascular coiling in 2143 patients with ruptured intracranial aneurysms: a randomised comparison of effects on survival, dependency, seizures, rebleeding, subgroups, and aneurysm occlusion.** *Lancet* 2005;366:809–17
2. Roy D, Milot G, Raymond J. **Endovascular treatment of unruptured aneurysms.** *Stroke* 2001;32:1998–2004
3. Im SH, Han MH, Kwon OK, et al. **Endovascular coil embolization of 435 small asymptomatic unruptured intracranial aneurysms: procedural morbidity and patient outcome.** *AJNR Am J Neuroradiol* 2009;30:79–84
4. Peluso JP, van Rooij WJ, Sluzewski M, et al. **Coiling of basilar tip aneurysms: results in 154 consecutive patients with emphasis on recurrent haemorrhage and re-treatment during mid- and long-term follow-up.** *J Neurol Neurosurg Psychiatry* 2008;79:706–11. Epub 2007 Sep 10
5. Sluzewski M, Menovsky T, van Rooij WJ, et al. **Coiling of very large or giant cerebral aneurysms: long-term clinical and serial angiographic results.** *AJNR Am J Neuroradiol* 2003;24:257–62
6. Willinsky RA, Taylor SM, TerBrugge K, et al. **Neurologic complications of cerebral angiography: prospective analysis of 2,899 procedures and review of the literature.** *Radiology* 2003;227:522–28
7. Kaufmann TJ, Huston J 3rd, Mandrekar JN, et al. **Complications of diagnostic cerebral angiography: evaluation of 19,826 consecutive patients.** *Radiology* 2007;243:812–19
8. Sprengers ME, Schaafsma JD, van Rooij WJ, et al. **Evaluation of the occlusion status of coiled intracranial aneurysms with MR angiography at 3T: is contrast enhancement necessary?** *AJNR Am J Neuroradiol* 2009;30:1665–71
9. Kaufmann TJ, Huston J 3rd, Cloft HJ, et al. **A prospective trial of 3T and 1.5T time-of-flight and contrast-enhanced MR angiography in the follow-up of coiled intracranial aneurysms.** *AJNR Am J Neuroradiol* 2010;31:912–18
10. Shankar JJ, Lum C, Parikh N, et al. **Long-term prospective follow-up of intracranial aneurysms treated with endovascular coiling using contrast-enhanced MR angiography.** *AJNR Am J Neuroradiol* 2010;31:1211–15. Epub 2010 Mar 25
11. Wallace RC, Karis JP, Partovi S, et al. **Noninvasive imaging of treated cerebral aneurysms. Part II. CT angiographic follow-up of surgically clipped aneurysms.** *AJNR Am J Neuroradiol* 2007;28:1207–12
12. Richter G, Engelhorn T, Struffert T, et al. **Flat panel detector angiographic CT for stent-assisted coil embolization of broad-based cerebral aneurysms.** *AJNR Am J Neuroradiol* 2007;28:1902–08
13. Masaryk AM, Frayne R, Unal O, et al. **Utility of CT angiography and MR angiography for the follow-up of experimental aneurysms treated with stents or Guglielmi detachable coils.** *AJNR Am J Neuroradiol* 2000;21:1523–31
14. Kovacs A, Flacke S, Tschampa H, et al. **Gated multidetector computed tomography: a technique to reduce intracranial aneurysm clip and coil artifacts.** *Clin Neuroradiol* 2010;20:99–107. Epub 2010 May 21
15. McCoy MR, Cruise GM, Killer M. **Angiographic and artefact-free computed tomography imaging of experimental aneurysms embolised with hydrogel filaments.** *Eur Radiol* 2010;20:870–76. Epub 2009 Sep 16
16. Forrest MD, O'Reilly GV. **Production of experimental aneurysms at a surgically created arterial bifurcation.** *AJNR Am J Neuroradiol* 1989;10:400–02
17. Constant MJ, Keeley EM, Cruise GM. **Preparation, characterization, and evaluation of radiopaque hydrogel filaments for endovascular embolization.** *J Biomed Mater Res B Appl Biomater* 2009;89:306–13
18. Cruise GM, Shum JC, Plenk H Jr. **Hydrogel-coated and platinum coils for intracranial aneurysm embolization compared in three experimental models using computerized angiographic and histologic morphometry.** *J Mater Chem* 2007;17:3965–73
19. Hanley M, Zenzen WJ, Brown MD, et al. **Comparing the accuracy of digital subtraction angiography, CT angiography and MR angiography at estimating the volume of cerebral aneurysms.** *Interv Neuroradiol* 2008;14:173–77
20. Pötin M, Gailloud P, Bidaut L, et al. **CT angiography, MR angiography and rotational digital subtraction angiography for volumetric assessment of intracranial aneurysms: an experimental study.** *Neuroradiology* 2003;45:404–09